Electronic Supplementary Material (ESI) for Nanoscale.

Supporting Information for:

Strain Engineering of van-der-Waals Heterostructures

Paul A. Vermeulen, Jefta Mulder, Jamo Momand, Bart J. Kooi

Zernike Institute for Advanced Materials, University of Groningen, Nijenborgh 4, 9747 AG Groningen, The Netherlands

1. Two-step growth method

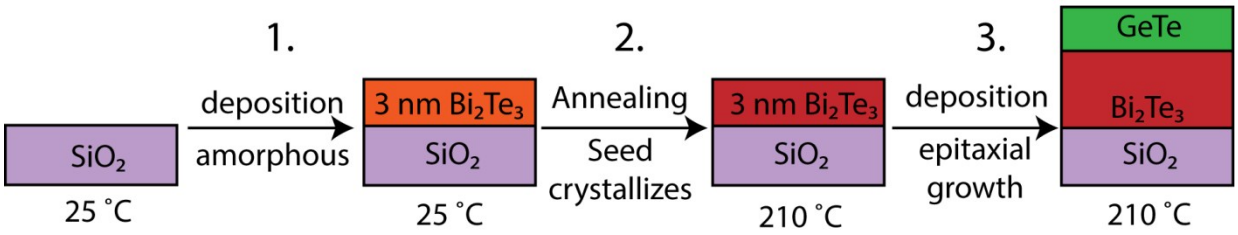

Figure S1. Using a 2-step growth method, flat, textured, stoichiometric films can be grown.[1] **First a thin (3nm) 'seed' layer of the desired film material (Bi_2Te_3 or Sb_2Te_3) was grown at room temperature (1), and heated with 5 K/min to 210 °C, which induces self-organized growth with c-axis out of plane even on an amorphous SiO_x substrate (2). Growth is immediately continued at 210 °C to prevent excessive evaporation. Due to vdWaals epitaxy, subsequent layers adopt the texture of the seed layer (3).**

2. Observed Reflections in RHEED and TEM Diffraction

The RHEED images were analyzed by obtaining an intensity line profile across the RHEED streaks. The intensity peak locations were determined by fitting a Gaussian function, and the peak separation of all detected peaks was fitted to a linear profile using a least squares fit. From this fit the streak spacing (in pixels) was extracted. The camera pixel spacing was calibrated using the literature bulk value of the relevant material and under the assumption that only the planes shown in figure S2 were in a reflection condition. The spacing of the first material layer, just before switching to a different material was taken for calibration, since this is the layer which is closest to bulk equilibrium.

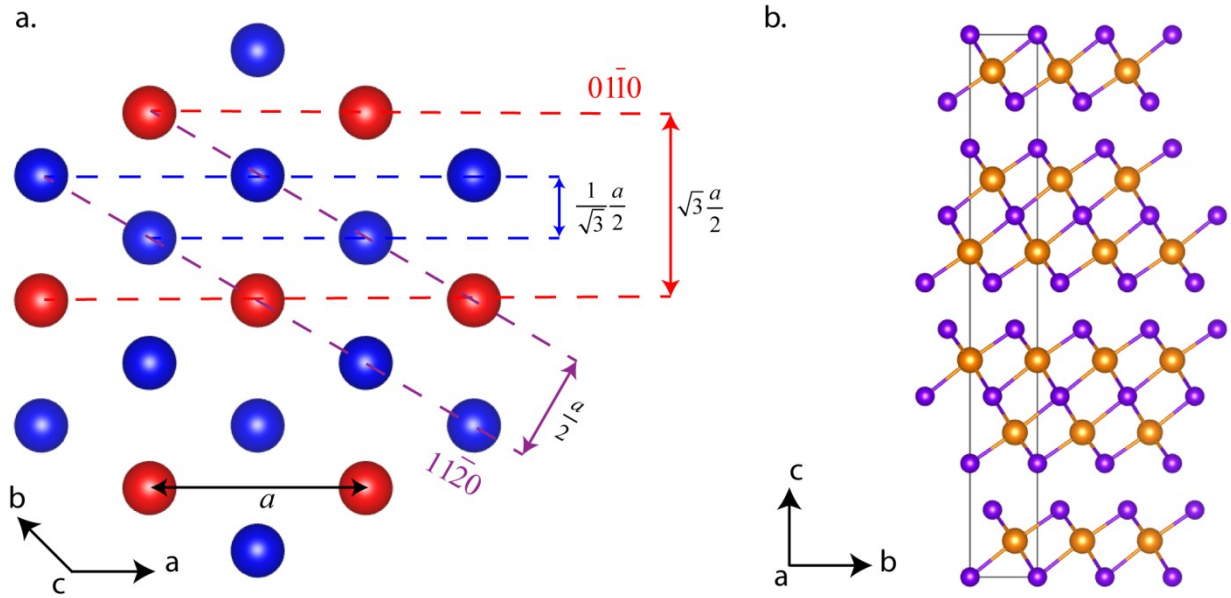

Figure S2. a.) The red atoms indicate the positions of the atoms in the outermost surface layer in Bi_2Te_3 and Sb_2Te_3 when grown with c-axis-up texture, the blue atoms the subsurface layer positions. Since the RHEED beam penetrates ~1nm, the shorter-scale symmetry is not probed, and the red {01-10} and purple {11-20} plane spacings are observed as streaks on the phosphor screen. The peaks are also marked accordingly in figure 1 of the main paper. In TEM diffraction, the beam penetrates through the whole sample, and the smaller scale symmetry is probed. The {01-10} reflection then becomes forbidden due to the intermediate planes at 1/3 spacing (blue) and the prevailing reflection becomes {03-30}. The {11-20} spacing is unaffected. Due to the trigonal symmetry of the structure, this means the ratio between both allowed reflections stays √3. b.) The R-3m symmetry structure of Bi_2Te_3 and Sb_2Te_3. Purple indicates the tellurium (Te) atoms, orange the antimony (Sb) or bismuth (Bi) atoms. Van-der-Waals-gaps occur every 5 atomic layers (one quintuple) and are bounded by a Te layer on both sides.

3. Cross-section TEM versus Plan-View EDS.

By measuring individual layer thicknesses from cross-section TEM images, one can calculate the overall elemental composition of the film when assuming stoichiometric Bi_2Te_3, GeTe and Sb_2Te_3 films. These values are compared to those obtained using Electron Dispersive Spectroscopy EDS scans of large (few micron) sized areas. The results are shown in table S1. The two types of measurements are considered to be in good agreement, which means no significant intermixing has occurred during growth. This is in agreement with the reports by Lanius et al. [2]

Bi_2Te_3/GeTe	Cross (at.%)	EDS (at.%)	Sb_2Te3/Bi_2Te_3	Cross (at.%)	EDS (at.%)
Bi	23.5	26.1	Bi	19.8	18.7
Ge	20.6	18.7	Sb	20.2	18.8
Te	55.9	55.3	Te	60.0	62.5

Table S1. Elemental composition from cross-section thickness measurement is indicated by "Cross." Composition from EDS scans is denoted by "EDS". The composition is shown per constituent element. The independent measurements agree within a reasonable error of 2 at.%.

4. Dislocation Movement

As discussed in the main text, a likely mechanism for strain relaxation is dislocation movement. In (isotropic) 3D Materials, it is energetically favourable for dislocations to glide to the interface, where strain is highest. The amount of broken bonds at the dislocation core remains the same. For 2D materials however, a dislocation core will generally be situated at the vdWaals gap. Glide to the strained interface involves severing covalent bonds within the quintuple layer. This is energetically unfavourable, so the dislocation is blocked and can only slide parallel to the strained interface. This mechanism could (partly) explain the persistence of a strain gradient in 2D materials.

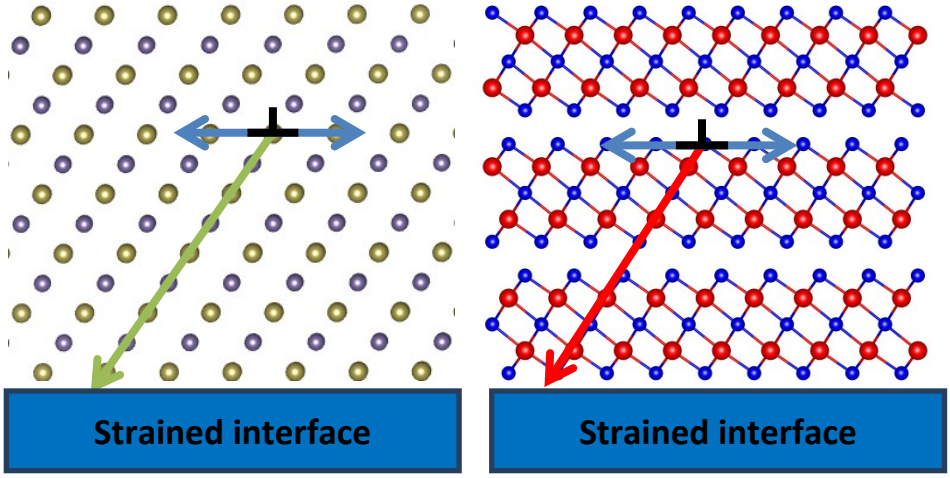

Figure S3. Comparison of Dislocation mobility in 3D materials (left) and 2D materials (Right). In 3D materials, dislocations are expected to glide to the interface and form a regularly spaced array, relieving strain in the film. In 2D materials, dislocations are expected to be confined to the height where they originally were introduced: only the layers are relaxed.

5. Model for Strain Relaxation

We propose a model for predictive control of the strain state of a quasi-2D bonded vdWaals multilayer, where we describe a strain ε in a growing (quintuple) layer as an overdamped harmonic oscillator.

$$\frac{d^2\varepsilon}{dh^2} = C\varepsilon - \beta\frac{d\varepsilon}{dh} \quad (1)$$

The rate of change of strain (LHS of eq. 1) is obtained by adding all forces/stresses acting on the growing layer, which are described on the RHS. The driving force for strain relaxation is given using Hooke's law $\sigma_{ij} = C_{ijkl}\varepsilon_{kl}$, which describes stress as linearly related to the strain through the general stiffness tensor C_{ijkl}.[3,4] This stress is the restoring force (first RHS term) of the oscillator. A damping term is added to eq.1 to account for the relaxation retardation force due to inter-layer vdWaals bonding and formation energy of dislocations. These effects are dependent on the lattice mismatch between consecutive (quintuple) layers, which is equivalent to the change in strain over height *h*: $d\varepsilon / dh$. Since lattice mismatch increases the length of the Te-Te vdWaals bonds beyond equilibrium, this increases the energy of the system. Furthermore, the number of dislocations necessary to accommodate this mismatch is also linearly dependent on the lattice mismatch. Both damping terms are therefore combined in the second RHS term with an unknown prefactor β. Eq.1 can be solved for strain as a function of thickness:

$$\varepsilon(h) = Ae^{-bh} \quad (2)$$

Where *A* is just a normalization constant, and *b* gives the rate of strain relaxation. The solutions of the harmonic oscillator contain a solution for an overdamped system, where the system returns with exponential decay to the equilibrium position:

$$\varepsilon = e^{bh} \text{ with } b = \frac{1}{2}(-\beta \pm \sqrt{\beta^2 - 4C})$$

Which is overdamped (valid) for $\beta^2 - 4C > 0$. (3)

Equation 2 can be fitted to the experimentally obtained lattice parameters, which will yield a value for *b*. The observed lattice parameters *α* at layer thickness *h* were fitted to an equation of the form:

$$\alpha = \alpha_f + \alpha_i e^{-bh} \quad (4)$$

Where absolute strain ε can be obtained by normalizing to the final lattice parameter $\alpha_f = \varepsilon(h = \infty)$

$$\varepsilon = \left|\frac{\alpha_i}{\alpha_f}\right| e^{-bh} = e^{-bh + \ln(\frac{\alpha_i}{\alpha_f})} \quad (5)$$

Since the prefactor $A = \alpha_i / \alpha_f$ is purely a scaling parameter which determines the strain at h = 0, it can be arbitrarily set to the desired strain value. The strain curves can be described from any hypothetical strained starting point. The defining parameter is the strain relaxation rate *b*.

The thickness for half strain h_f can be obtained:

$e^{-bh_f} = \frac{1}{2} e^{-bh_i}$, with $h_i = 0$, yields $h_f = \frac{Ln(2)}{b}$ (6)

Formula 3 can be rewritten to obtain $\beta = \frac{-b^2 - C}{b}$ Plugging in C = 50 GPa [5] (in-plane Youngs modulus) yields β = 500 GPa (b=0.1). This should be interpreted as the combination of pressures preventing relaxation, e.g. the interlayer vdWaals force and the dislocation formation potential.

6. **Dislocation Density Calculation**

Using the strain relaxation described by equation 2 of the main text, we can readily derive the dislocation density as a function of layer thickness. We note that this explicit model and formula is not strictly needed, and a numerical result can be obtained directly from the data. Since for 2D materials dislocations are not concentrated at the (strained) interface, two steps are added to calculate the dislocation density at arbitrary film height – which is then irrespective of actual film thickness. The dislocations considered here are always of edge-type with Burgers vector and line direction oriented in a plane parallel to the interface. Such edge dislocations are the most efficient in relaxing strain. A single array of dislocations can only relax the strain in one dimension however. Since the strain is bidirectional (in a plane parallel to the interface) a network of dislocations is required. Due to hexagonal symmetry of the individual telluride planes (parallel to interface) which are stacked in a-b-c fashion (perpendicular to the interface), it is expected that a triangular network of dislocation lines is present in planes parallel to the interface. The Burgers vectors have a size equal to the *a* lattice parameter (and are of 1/3<11-20> type).[6] For the present analysis it is sufficient to only consider a single plane spanned by the *a*-lattice vector parallel to the interface and the *c*-vector perpendicular to the interface, where the strain is relaxed in one dimension.

A step by step derivation is given below.

1. Strain is approximated using a decaying exponential:

$\varepsilon(h) = A e^{-bh}$

2. The number fraction of dislocations *N* in an area defined by the unit cell width *a* (parallel to interface) and between height zero and final height h (perpendicular to interface), is directly proportional to the strain, with ϵ_0 the strain at height zero (ϵ(0)):

$N = \epsilon_0 - \epsilon = \epsilon_0 - A e^{-bh}$

3. The total dislocation density δ_T (number of dislocations per unit of area *A*) is then given by:

$\delta_T = \frac{N}{A} = \frac{-A e^{-bh} + \epsilon_0}{a}$

For 2D materials dislocations will not move to the interface, and an additional step is required to calculate the dislocation density at arbitrary distance from the interface, for a given layer thickness.

4. To calculate the number of dislocations at arbitrary distance from the interface, for a given strain profile, we take the derivative of N, which gives the dislocation number at a given thickness.

$$n(h) = \frac{dN}{dh} = Abe^{-bh}$$

5. The dislocation number can again be normalized to a density:

$$\delta_{2D} = \frac{Abe^{-bh}}{a}$$

6. The relevant spacings between equidistantly spaced dislocations can trivially be obtained by

$$d = 1/\delta$$

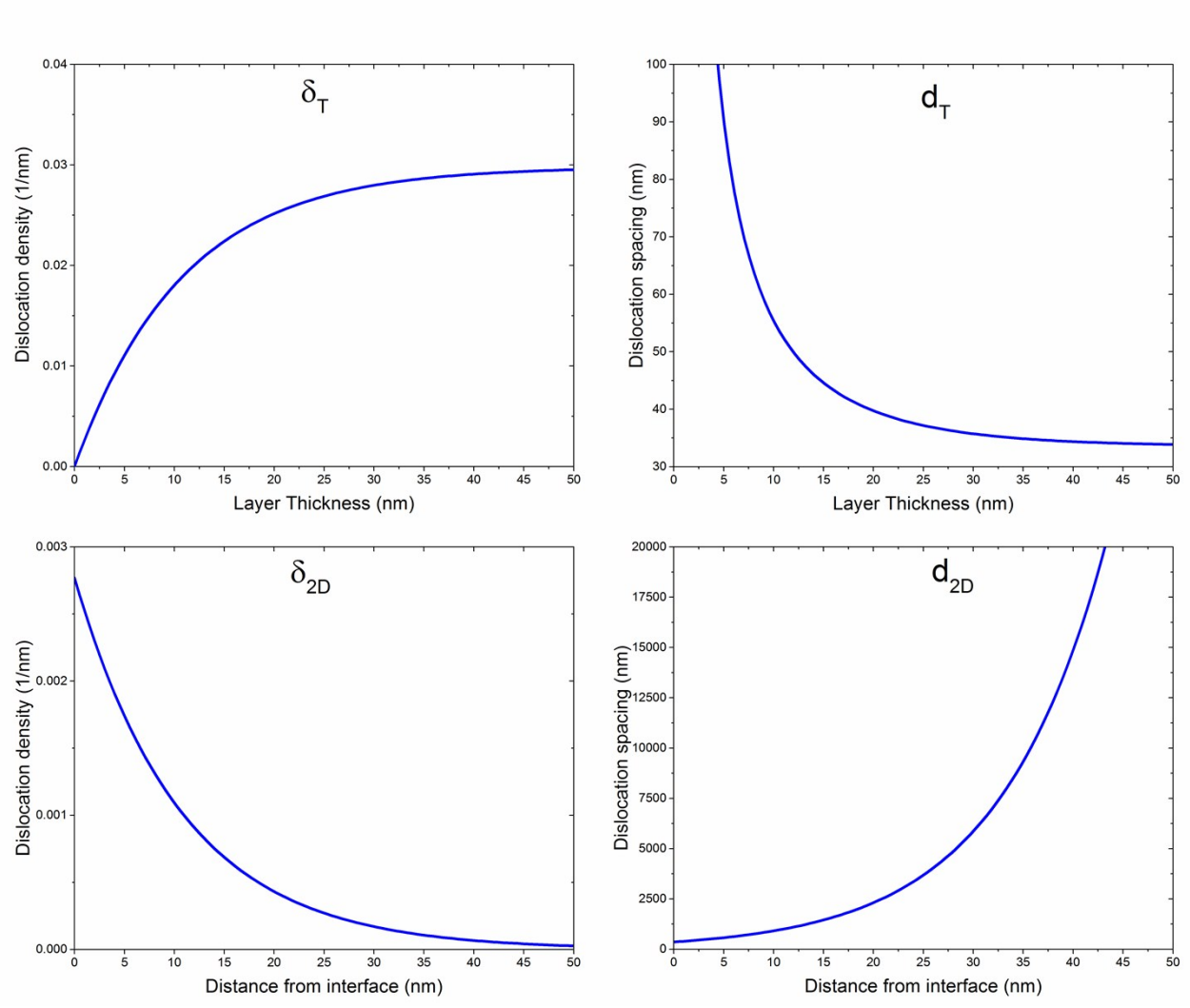

Figure S4. Dislocation densities per unit area in a cross section are plotted, assuming Sb_2Te_3 growth on Bi_2Te_3. A=0.127, b=0.0929, *a* = 4.26 nm. Top Left: Total dislocation density in the film (#/nm^2) versus film thickness (nm). Top Right: Distance (nm) in between equidistantly spaced dislocations versus film thickness when it is assumed that that the total dislocation density in the top left image translates to a single array of misfit dislocations at the interface, resembling the case of 3D materials where misfit is relaxed at the interface. Such a single array is rather hypothetical because it is inconsistent with the assumed exponentially decaying strain profile. Bottom Left: Dislocation density (#/nm^2) versus distance from the interface (nm) for 2D materials where dislocations are not localized at the interface. Bottom Right: Distance (nm) in between equidistantly spaced dislocations versus distance from the interface (nm). The dislocation concentration is still highest at the interface, but decaying for increasing height within the film. In contrast to the hypothetical top right image, this bottom right image displays an actual physical picture consistent with the exponential strain relaxation observed, which could be verified in for instance cross-sectional TEM images.

7. Plan-view TEM Imaging

TEM analysis of plan-view samples has been performed on bilayers of Sb_2Te_3 on Bi_2Te_3 (Figure S6ab) and GeTe on Bi_2Te_3 (Figure S6cd). The real-space images show that no regular moiré fringes appear, which would be the signature of a stacked system with 2 distinct lattice parameters. This indicates the strain gradient observed through RHEED still persists even in a TEM foil. The domain sizes of Sb_2Te_3 and GeTe are difficult to estimate, but it is clear the domain size in GeTe is significantly smaller, which can be seen from both the real-space image, and the diffraction rings, where for Sb_2Te_3 distinct spots belonging to a specific domain can be observed.

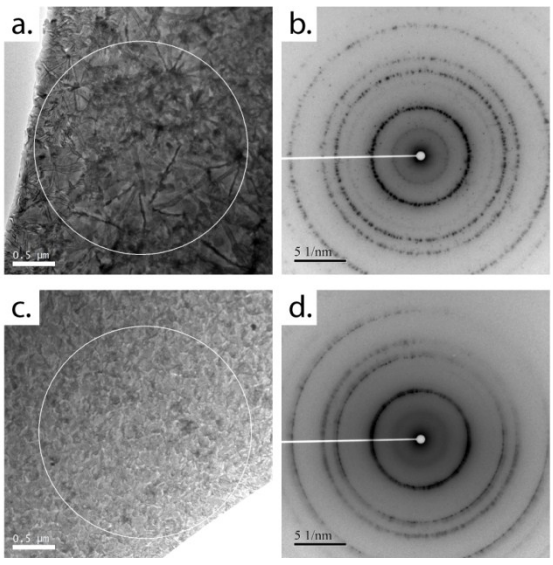

Figure S5. *ab* and *cd* show bilayers of Sb_2Te_3 on Bi_2Te_3 and GeTe on Bi_2Te_3 respectively. The layers were sufficiently thick to allow a full relaxation curve to be recorded with RHEED. *ac* show plan-view TEM,

revealing some regions with disordered moiré, and small domains in GeTe compared to Sb_2Te_3. *bd* Shows the diffraction patterns of *ac*, revealing broadened rings, with distinct spots visible for Sb_2Te_3 due to its larger domain size compared to the one for GeTe.

8. References

1 Y. Saito, P. Fons, L. Bolotov, N. Miyata, A. V. Kolobov and J. Tominaga, *AIP Adv.*, 2016, **6**, 2–7.

2 M. Lanius, J. Kampmeier, C. Weyrich, S. Kölling, M. Schall, P. Schüffelgen, E. Neumann, M. Luysberg, G. Mussler, P. M. Koenraad, T. Schaepers, D. Grützmacher, T. Schäpers and D. Grützmacher, *Cryst. Growth Des.*, 2016, **16**, 2057–2061.

3 H. Koc, *Jt. UFFC, EFTF PFM Symp.*, 2013, 41–44.

4 N. Ashcroft and D. Mermin, *Solid State Physics*, Harcourt, 1976 Colle., 1976.

5 B.-L. Huang and M. Kaviany, *Phys. Rev. B*, 2008, **77**, 1–19.

6 D. Hull and D. J. Bacon, *Introduction to Dislocations*, Elsevier, Fifth Edit., 1984.